Using a Fluorescent Cytosine Analogue tC o To Probe the Effect of the Y567 to Ala Substitution on the Preinsertion Steps of dNMP Incorporation by RB69 DNA Polymerase

ARTICLE *in* BIOCHEMISTRY · MAY 2012

Impact Factor: 3.02 · DOI: 10.1021/bi300241m · Source: PubMed

4 AUTHORS, INCLUDING:

William Konigsberg
Yale University
274 PUBLICATIONS **9,996** CITATIONS

SEE PROFILE

Published in final edited form as:
Biochemistry. 2012 June 5; 51(22): 4609–4617. doi:10.1021/bi300241m.

Using a Fluorescent Cytosine Analogue tC° to Probe the Effect of Y567 to Ala Substitution on the Pre-insertion Steps of dNMP Incorporation by RB69 DNA Polymerase†

Shuangluo Xia[§], **Jeff Beckman**[§,#], **Jimin Wang**, and **William H. Konigsberg**[*]
Department of Molecular Biophysics and Biochemistry, Yale University, New Haven, CT06520-8114, USA

Abstract

Residues in the Nascent Base-pair binding Pocket (NBP) of bacteriophage RB69 DNA polymerase (RB69pol) are responsible for base discrimination. Replacing Tyr567 with Ala leads to greater flexibility in the NBP, increasing the probability of misincorporation. We used the fluorescent cytosine analogue, 1,3-diaza-2-oxophenoxazine (tC°) to identify pre-insertion step(s) altered by NBP flexibility. When tC° is the templating base in a wild type (wt) RB69pol ternary complex, its fluorescence is quenched only in the presence of dGTP. However with the RB69pol Y567A mutant, tC° fluorescence is also quenched in the presence of dATP. We determined the crystal structure of the dATP/tC°-containing ternary complex of the RB69pol Y567A mutant at 1.9 Å resolution, and found that the incoming dATP formed two hydrogen bonds with an imino-tautomerized form of tC°. Stabilization of the dATP/tC° base-pair involved movement of the tC° backbone sugar into the DNA minor groove and required tilting of the tC° tricyclic ring to avoid a steric clash with L561. This structure, together with the pre-steady-state kinetic parameters and dNTP binding affinity, estimated from equilibrium fluorescence titrations, suggested that the flexibility of the NBP, provided by Y567 to Ala substitution, led to a more favorable isomerization step resulting in an increase in dNTP binding affinity.

Replication of a genome from any organism must occur with minimal mistakes if the progeny are to remain viable. Replicative DNA polymerases perform this task, making less than one mistake per 10^6 base-pairs synthesized.[1–4] Fidelity is increased by an additional 100-fold if the polymerase has exonuclease capability.[5–7] The number of errors made during replication depends on how well a DNA polymerase (pol) can recognize a dNTP as either correct or incorrect for pairing opposite the templating base. Sometimes a DNA pol can circumvent the geometric constraints imposed by residues in the Nascent Base-pair binding Pocket (NBP) so that incorrect dNTPs can be incorporated albeit with low efficiency.

Based on crystal structures and studies using fluorescent probes, selection of the correct dNTP most likely occurs prior to phosphoryl transfer.[8–16] Subsequent to dNTP binding (Scheme 1), the polymerase Fingers domain closes, aligning the reactive centers of the substrates, leading to rapid nucleotidyl transfer.[13, 17–19] The incorrect dNTP either fails to induce Fingers closing, or if the Fingers do close the result is an unstable, but potentially productive, ternary complex.[13, 20–21]

†This work was supported by NIH RO1-GM063276-09 (to W.H.K.) and by SCSB-GIST (to J.W.).

[*] Corresponding author: Prof. William H. Konigsberg SHM CE-14 Department of Molecular Biophysics and Biochemistry Yale University New Haven, CT 06520-8114 Telephone: (203) 785-4599 Fax: (203) 785-7979 william.konigsberg@yale.edu.
[§]These authors contributed equally to this work
[#]Present address: Genzyme Corporation, Cambridge, MA

DNA pols from different families, and even within families, differ greatly in their ability to resist insertion of incorrect dNTPs. The B family DNA pol from bacteriophage RB69 (RB69pol) maintains high fidelity even when it encounters damaged templates or templating base analogues.[22–28] Interestingly, upon substitution of Y567 with Ala in the NBP, the mutant RB69pol inserts incorrect dNTPs with efficiencies 10^2 to 10^3 fold greater than wild type (wt) pol.[29] Crystal structures of ternary complexes of the RB69pol Y567A mutant suggest that the reduction in base selectivity exhibited by this mutant was likely due to an increase in NBP flexibility, leading to stable conformations of the templating base even when paired opposite incorrect dNTPs, a situation that would otherwise be blocked in the wt enzyme.[15, 29] However, a fuller understanding of how increased flexibility of residues in the NBP affects base selectivity requires analysis of kinetic steps that occur prior to nucleotidyl transfer. For this purpose we employed the highly fluorescent 1,3-diaza-2-oxophenoxazine (tC°) to probe the pre-insertion steps before chemistry. As shown in Fig 1, tC° is a tricyclic cytosine analogue. When presents as the templating base, it can be used to follow isomerization of DNA pols from an open to a closed conformation in response to binding of an incoming dNTP.[12, 14] Furthermore, unlike 2-aminopurine (2AP), a well-characterized fluorescent adenine analogue, where fluorescence quenching is totally dependent on base stacking, quenching of tC° fluorescence depends on the formation of hydrogen bonds (HB) with the templating base.[30–34] Sandin et al reported that tC° base pairs exclusively with guanine (G) and caused minimal perturbations in the structure of duplex DNA.[35–36] Kuchta's lab has recently discovered that tC° triphosphate (dtC°TP) is preferentially inserted opposite templating G and A residues by both KF and human DNA pol alpha.[37] They speculated that the incorporation of dAMP opposite tC° and vice-versa was due to the propensity of tC° to tautomerize into its imino form (Fig. 1).[37]

We found that tC° fluorescence was quenched only when paired opposite dGTP in a wt RB69pol ternary complex, reflecting formation of a stable nascent base-pair.[15] Surprisingly, we found that the net equilibrium dissociation constant ($K_{d,net}$) for dGTP binding opposite tC° with the Y567A mutant, in the absence of chemistry, was reduced by more than 200 fold relative to the corresponding wt ternary complex. In addition, dATP was able to form a stable nascent base-pair with tC° only with the Y567A mutant. To gain further insight into why this mutant has increased affinity for dGTP and was permissive for dATP binding, we determined the crystal structures of the dGTP/tC° and dATP/tC°-containing ternary complexes of the RB69pol Y567A mutant at 1.9 Å resolution. We found that incoming dATP formed two HBs with an imino-tautomerized form of tC°. However, stabilization of the dATP/tC° base-pair required: (i) movement of the tC° backbone sugar into the DNA minor groove; (ii) lateral shifting of residues A567 and G568 toward residue Y416; (iii) tilting of the tricyclic ring of tC° base to avoid a steric clash with L561. Together, these data suggest that flexibility of the NBP provided by replacement of Y567 with Ala, led to a more favorable isomerization step (higher k_2 value compared to the k_2 exhibited by wt pol, as shown in Scheme 1) resulting in an increase in substrate binding affinity.

EXPERIMENTAL PROCEDURES

Materials

Materials and reagents were of the highest quality commercially available. dNTPs were purchased from Roche (Burgess Hill, UK), T4 polynucleotide kinase was purchased from New England Biolabs (Ipswich, MA), and [γ-32P]ATP was purchased from MP Biomedicals (Irvine, CA).

Enzymes

Wild-type RB69pol and the Y567A mutant, in an exonuclease-deficient background (D222A and D327A), were over-expressed in *E. coli* strain BL21(DE), purified, and stored as previously described.[38–41]

DNA Substrates

The sequence of the primer-template (P/T) used in this study was as follows: 5'-GCGGACTGCTTAC and 5'-TCA(tC°)GTAAGCAGTCCGCG. A dideoxy-terminated primer (ddC at 3' end of primer strand) was used for structural work, fluorescence titrations and stopped-flow fluorescence experiments. Oligonucleotides were synthesized at the Keck facilities (Yale University). The tC° phohphoramidite was purchased from Glenn Research Inc (Sterling, VA). The primer was labeled at the 5'-end with ^{32}P using T4 polynucleotide kinase and [γ-32P]-ATP and annealed to unlabeled templates as previously described.[42–43]

Equilibrium fluorescence titrations

Fluorescence emission spectra with 300 nM dideoxy-terminated P/T (tC° at the n position of template strand) with wt or the Y567A mutant (1 μM) and 66 mM Tris-HCl (pH 7.4) and 10 mM $MgSO_4$ were acquired at 23°C with a Photon Technology International (PTI) scanning spectrofluorometer. Spectra were acquired by exciting the sample at 364 nm, and collecting emission from 380 to 700 nm. The intensities were corrected for the intrinsic fluorescence of the enzyme and buffer solutions.

Stopped-flow fluorescence experiments

These experiments were carried as described previously except that tC° was used in place of 2AP.[14] The excitation and emission wavelengths for tC° are 364 nm and 450 nm respectively. The final reaction mixtures consisted of 50 mM Tris (pH7.4), 10 mM $MgCl_2$, 200 nM P/T, 2 μM RB69pol, and varying dGTP concentrations.

Chemical Quench Experiments

Rapid chemical quench experiments were performed at 23°C with a buffer solution of 66 mM Tris-HCl (pH 7.4) using a Kintek RFQ-3 instrument. For k_{pol} and $K_{d,app}$ determinations, single-turnover conditions were used with a 10-fold excess RB69pol over P/T. Briefly, enzyme and P/T from one syringe were rapidly mixed with Mg^{2+} and various [dNTP] from the other syringe for times ranging from 5 ms to 1 min. The final concentrations after mixing were 1 μM enzyme, 90 nM ^{32}P-labeled P/T, and 10 mM Mg^{2+}. In addition, 10×[cold P/T]/[enzyme] was used to ensure that single-turnover conditions were met. Reaction mixtures were quenched with 0.5 M EDTA (pH 8.0). Substrates and products were separated by PAGE (19:1, w/v, acrylamide:bisacrylamide gels containing 8M urea), visualized using a STORM imager (Molecular Imaging), and quantitated using Imagequant (GE Healthcare).

Data Analysis

The amount of product formed versus time for each [dNTP] were fitted by nonlinear regression to a single exponential equation: $Y = A[1-\exp(-k_{obs*}t)]+C$ to obtain observed rates of product formation, where Y is the concentration of the DNA product formed during the reaction, C is the offset constant. The kinetic parameters k_{pol} (the rate of maximum nucleotide transfer) and $K_{d,app}$ (defined as the [dNTP] at which the rate of phosphoryl transfer reaches 1/2 k_{pol}), were obtained by plotting k_{obs} versus [dNTP] to a hyperbolic equation: $k_{obs} = k_{pol}$ [dNTP]/($K_{d,app}$ + [dNTP]), where k_{obs} represents the observed rate at a given [dNTP]. Note that the $K_{d,app}$ values are not ground-state dissociation constants for dNTP binding. This is because the observed [dNTP]-dependence of rates of product

formation is affected by steps such as the reversible conformational change that occurs subsequent to dNTP binding but prior to phosphoryl transfer.

Crystallization of Y567ARB69pol ternary complexes with dATP/tC° or dGTP/tC°

A 13mer dideoxy terminated primer annealed to a 18mer template strand was used for crystallization. The RB69pol Y567A mutant (120 μM final concentration) was mixed with an equimolar ratio of freshly annealed P/T, dATP was then added to give a final concentration of 2 mM. Using micro-batch vapor-diffusion methods, a solution of 100 mM $CaCl_2$, 15% (w/v) PEG 350 monomethyl ether (MME), and 100 mM sodium cacodylate (pH 6.5) was mixed with an equal volume of the protein complex. Crystals typically grew in 2 days at 20°C with dimensions of about 100 μm × 120 μm × 150 μm. Crystals were transferred from the mother liquor to a cryoprotectant/precipitant stabilization solution containing 20% (w/v) PEG 350 MME, 100 mM $CaCl_2$, and 100 mM sodium cacodylate (pH 6.5), then to the stabilization solution with PEG 350 increased to 30% (w/v) as a cryoprotectant prior to freezing in liquid nitrogen.

Data collection, structure determination, and refinement

X-ray diffraction data were collected using synchrotron radiation sources at beam line 24ID-E, Northeast Collaborative Access Team (NECAT), Advanced Photon Source, Argonne National Laboratory (APS, ANL, Chicago, IL) at a wavelength of 0.979 Å and at 110 K. The crystal belonged to the orthorhombic space group $P2_12_12_1$ with different unit cell parameters (Table 1). Data were processed using the HKL2000 program suites.[44]

The structure was solved by molecular replacement using AMORE, starting with the pol structure from the ternary complex of wt RB69pol without the P/T duplex or dNTP,[15] and refined using REFMAC5.[45–46] The P/T duplex and dNTP were built into electron density maps using the program COOT.[47] Structure refinement statistics are summarized in Table 1. Figures depicting the crystal structures were made using the program Pymol.[48]

PDB accession numbers

Coordinates and structure factors for the dATP/tC° and dGTP/tC°-containing ternary complex of Y567A RB69pol have been deposited in the Protein Data Bank under accession code 3QNO and 3QNN respectively.

RESULTS AND DISSCUSION

Incorporation of dGMP and dAMP opposite tC° by wt RB69pol and the Y567A Mutant

Although we had previously shown that the Y567A mutant incorporated incorrect dNMPs more efficiently than wt RB69pol, we were interested in determining how this pol mutant and wt RB69pol would process correct and incorrect incoming dNTPs opposite a templating tC°, a fluorescent analogue of cytosine. Accordingly, we determined the pre-steady-state kinetic parameters for dGMP and dAMP incorporation opposite tC° by wt RB69pol and the RB69pol Y567A mutant. As shown in Table 2, insertion of dGMP opposite tC° by wt RB69pol was very efficient, with a $k_{pol}/K_{d,app}$ value of 1.8 $\mu M^{-1}s^{-1}$, which is comparable to the incorporation efficiency of dGMP opposite dC (2.9 $\mu M^{-1}s^{-1}$) as reported previously.[38] In contrast, the insertion of dAMP opposite tC° by wt RB69pol was 500 fold less efficient than dGMP, with a $k_{pol}/K_{d,app}$ value of 3.5 $\times 10^{-3}$ $\mu M^{-1}s^{-1}$ (Table 2 and Fig. 2). By replacing Y567 with Ala, the incorporation efficiency of dGMP and dAMP opposite tC° increased 24-old and 200-fold respectively (Table 2 and Fig. 2). The 24-fold increase in dGMP incorporation efficiency by the Y567A mutant was mainly due to a 35-fold decrease in $K_{d,app}$ (4 μM versus 140 μM for wt). While the dramatic increase in dAMP incorporation efficiency by the Y567A mutant was the result of a large increase in k_{pol} (180 s^{-1} versus 6

s^{-1} for wt) and a large decrease in $K_{d,app}$ (270 μM versus 1700 μM for wt) (Table 2). In addition, the maximum turn-over rates for insertion dGMP and dAMP opposite tC° by the Y567A mutant were almost identical, in contrast to the 40-fold difference in k_{pol} observed with wt RB69pol.

Net binding affinity of dGMP or dAMP opposite a templating tC° in a RB69 ternary complex

The value of $K_{d,app}$ determined from our pre-steady state kinetics experiments was an estimate of the net equilibrium dissociation constant, $K_{d,net} = K_{d,1}/(1+K_2)$, where $K_{d,1}$ is the ground state binding constant and K_2 is the equilibrium constant for the isomerization step (ED_ndNTP to FD_ndNTP) according to scheme 1. Since the fluorescence of tC° is very sensitive to its local environment, we designed a P/T duplex with a dideoxy- terminated ddC at the 3' end of the primer to measure the net binding affinity of dNTPs opposite tC°. Upon addition of a 1mM concentration of each of the four dNTPs to the wt RB69pol-P/T binary complex, only dGTP quenched the fluorescence of tC° (by about 30%). In contrast, both dGTP and dATP quenched tC° fluorescence, when added to the Y567A-P/T binary complex (by approximately 30% and 15%, respectively). As shown in Table 3, the $K_{d,net}$ for dGTP with the wt RB69pol-P/T binary complex was 110 μM, which is comparable to the $K_{d,app}$ of 170 μM, determined by single turnover experiments. Binding of dGTP to the Y567A-P/T binary complex gave a much lower $K_{d,net}$ (0.5 μM), whereas dATP gave a $K_{d,net}$ of 100 μM (Table 3). Thus, substitution of Y567A with Ala decreased the $K_{d,net}$ of dGTP to the pol-P/T binary complex by 220 fold.

As an independent check of these results, the $K_{d,net}$ for dGTP binding to the wt RB69pol-P/T binary complex was estimated using stopped-flow fluorescence. Various [dGTP] were rapidly mixed with the wt RB69pol-P/T binary complex, resulting in a series of time-courses for tC° fluorescence quenching. When the fluorescence amplitude change was plotted against [dGTP] (Fig. 3D), a $K_{d,net}$ of 170 μM was obtained which was comparable to the $K_{d,net}$ value determined by equilibrium fluorescence titration (110 μM). Surprisingly, full quenching of tC° fluorescence occurred within the instrument dead-time (< 2 ms), indicating that the rate of quenching was greater than 500 s^{-1}. This value was at least as fast as the rate of Fingers closing as estimated previously by the rate of 2AP fluorescence quenching.[49]

Crystal structures of the Y567A RB69pol mutant in complex with a dideoxy P/T containing a templating tC° opposite dGTP and dATP

For further insight into how the Y567A mutant was able to insert dGTP or dATP opposite tC° with such high efficiency, we determined two crystal structures of the Y567A mutant in ternary complexes with dGTP/tC° and dATP/tC° nascent base-pairs at 1.92 Å and 1.88 Å with free R factors of 21.3% and 21.2% respectively (Table 1). Both structures were nearly identical with Cα root mean square deviations (RMSDs) of about 0.12 Å. The network of ordered water molecules, particularly those in the vicinity of the NBP, could be clearly visualized due to the high-resolution obtained with these crystals. As shown in Fig 4, there are three hydrogen bonds formed between the incoming dGTP and tC°, as expected. In contrast, two hydrogen bonds were observed between the incoming dATP and what is likely to be the imino-tautomer of tC°. Otherwise, with the amino-tautomer there would be a steric clash between the N6-H of adenine and N7-H of the amino-tautomer of tC° as the inter-atomic distance between the two nitrogen atoms is 3.1 Å. The inter-atomic distance between N1 of adenine and N3 of tC° was 2.7 Å. This observation is consistent with prediction by Kuchta et al[37] that the imino-tautomer of tC° and adenine presumably forms a base-pair that is isosteric with a dT/dA base pair.

By superimposing the palm domains of the structure of the dATP/tC°-containing Y567A RB69pol ternary complex with that of the 1.8 Å resolution structure of the dCTP/dG-

containing wt ternary complex,[15] it appeared that the A567 and G568 residues in the Y567A mutant shifted laterally toward the Y416 side chain, and vertically into the DNA minor groove by approximately 0.7 and 0.4 Å, respectively, compared to their positions in the wt structure (Fig. 5A). In addition, the sugar moiety of the templating tC° shifted by a similar distance so that interaction between G568 and tC° in the Y567A mutant are similar to those between G568 and the templating dC in the wt enzyme (Fig 5A). Presumably, the movement of the sugar backbone into the space provided by the shifting of residues A567 and G568 prevented a potential steric clash of the tC° tricyclic ring with the side chain of L561 (Fig. 6A). However, this movement caused the tC° base to tilt slightly towards the penultimate base-pair at the P/T junction creating a slight twist in the dATP/tC° nascent base-pair geometry (Fig. 6A). Also, the O2 of tC° overlays nicely with the N3 of guanine when paired with an incoming dCTP mimicking Watson-Crick like geometry. When the dGTP/tC°-containing Y567A mutant structure was superimposed on the dCTP/dG-containing wt structure, similar shifts of A567 and G568 were observed (Fig. 5B). Again, the tricyclic ring of tC° tilted towards the duplex DNA avoiding a clash with the side chain of L561 (Fig. 6B). The downward movement of the sugar moiety of the templating tC°, and the lateral shift of residues A567 and G568 cannot occur in the wt RB69pol due to the rigidity of the NBP. This could explain why the incorporation efficiency of dGMP and dAMP opposite tC° increased dramatically upon substitution of Y567 with Ala.

In the structure of the dATP/tC°-containing Y567A RB69pol ternary complex, there are two alternative conformations of the 5' template strand overhang (Fig. 7). In one conformation, the base of dC at the n+2 position of the template strand was stacked on top of the dA base at the n+1 position in the template. In the other conformation, dC at the n+2 position of template was flipped back into the NBP, forming a Hoogsteen base-pair with dG at n-1 of the template strand (Fig. 7). This backward flip of dC at n+2 of the template was also stabilized by π-π interactions between tC° and base of dC at the n+2 position (Fig. 7). The occupancy of this alternative conformation of 5'-template overhang in the dGTP/tC°-containing Y567A ternary complex was much lower than in the dATP/tC°-containing Y567A ternary complex so that it was nearly unobservable.

Tautomerization of tC° in the Y567A mutant ternary complex

Our structural data suggests that a potential steric clash would occur between L561 and tC° that could cause the dATP/tC° nascent base-pair in the wt RB69pol ternary complex to be rejected if the side chain of L561 cannot adopt an alternative rotamer conformation. Another possible interpretation for the kinetic behavior of wt RB69pol, with respect to the insertion of dAMP opposite tC°, is that the rigidity of the NBP of wt RB69pol prevents tautomerization of tC° within the ternary complex. It has been reported that unmodified cytosine exists mainly as the amino-tautomer in solution with an estimated amino to imino ratio of 10^4 to 1.[37] Thus, it is likely that the amino-tautomeric form of tC° is more highly populated than the imino form both in solution and presumably within the initial collision complex. Upon formation of the closed ternary complex, interactions between the enzyme and the dATP/ tC° pair stabilizes the imino form of tC°, shifting the equilibrium toward the imino form. Due to the flexibility of the NBP in the Y567A mutant, the amino to imino conversion occurs within the closed ternary complex so that we have captured the imino form of tC°. In contrast, for wt RB69pol, the rigidity of the NPB creates a much higher energy barrier for this conversion so that it is unlikely to occur. The resulting amino-tautomer of tC°/dATP wobble base pair causes a steric clash with Y567 and L561 of the NBP with wt RB69pol and would be rejected from the ternary complex. Possibly, the prevention of the amino to imino conversion by wt RB69pol could be a general mechanism for rejecting minor tautomers of mispaired bases.

Increased flexibility of the NBP leads to a more favorable forward isomerization step

Previous work by several groups, using fluorescent probes attached to either the DNA pol or as fluorescent DNA bases have shown that dNTP selection by DNA pols including those from T7, Klentaq, KF, T4 and RB69 likely occurs prior to or during formation of the closed ternary complex.[10, 13–14, 22, 50–51] Our stopped-flow fluorescence experiments showed that binding of dGTP opposite tC° in the NBP of wt or the Y567A RB69pol mutant led to very rapid quenching of tC° fluorescence (> 500 s^{-1}). This suggested that the formation of a stable dGTP/tC° nascent base-pair, including proper alignment of reactive groups and catalytic residues, occurs concomitantly with Fingers closing into a closed, pre-insertion complex. Both pre-steady state kinetic experiments and fluorescence titration experiments show that the $K_{d,app}$ and $K_{d,net}$ for both dGTP and dATP decrease dramatically upon replacing Y567 with Ala. According to scheme 1, the $K_{d,net}$ is defined as $K_{d,1}/(1+K_2)$. It is unlikely that the Y567A mutation would influence the initial collision complex formation ($K_{d,1}$). Therefore, a more favorable forward commitment must be controlled by K_2 with the mutant enzyme. This could be due to a more rapid forward rate constant (k_2) relative to the wt enzyme due to increased NBP flexibility resulting from the Y567 to Ala substitution. This notion is supported by our structural data showing that a downward movement of the sugar moiety of the templating tC°, and the lateral shifting of residues A567 and G568 occurred with the Y567A mutant but not with wt RB69pol. It is also consistent with our previously reported structures of dCTP/dG-containing ternary complexes of wt RB69pol and Y567A mutant which showed that an inter-residue HB between Y567 and Y391 is responsible for helix P and residue G568 being in a strained geometry.[15] By disruption this HB interaction by the Y567 to Ala substituion, G568 was able to relax into a new position with both the dCTP/dG and dTTP/dG pairs. Our observations provide an example of how an increase in substrate binding affinity can result from an increase in k_2.

tC° can potentially be used as a probe for monitoring conformational changes in other DNA pols

Because the NBP of all B family replicative pols contain highly conserved residues,[52] including a Tyr at a position analogous to 567 in RB69pol, we propose that this correlation between rigidity and base selectivity is likely to be generally applicable to pols in the B family. Thus it appears that tC° is a useful templating base analogue to test the effect of amino acid substitutions on NBP flexibility in other B family pols, because it detects the formation of stable nascent base-pairs. In addition, tC° can also be used in determining kinetic parameters of pre-insertion steps within the catalytic cycle. However its potential was limited in the case of RB69pol, because the forward rate constants for formation of a closed ternary complex are too large to determine accurately using our stopped-flow fluorescence instrument. Some replicative DNA pols, such as T7 DNA pol,[13] isomerize to the active ternary complex more slowly, and therefore are able to provide the desired data for the rates of Fingers closing.

In summary, increasing the flexibility of amino acid residues on the DNA minor groove side of the NBP in the Y567A mutant leads to highly efficient insertion of incorrect dNTPs. Data provided by analysis of tC° fluorescence quenching and crystal structures reveal that the increased flexibility provided by the Y567A mutant has the effect of increasing the stability of the ternary complex following the pre-insertion isomerization step by helping tC° avoid a steric clash with L561 as it shifts down toward the templating tC° base to form a closed ternary complex. Finally, the data also shows that L561 in wt RB69pol is rigid, along with G568 and A569, and that these three residues form a network that prevents unnaturally large templating base analogues from forming stable interactions with incoming dNTPs.

Acknowledgments

We thank the staff of the NE-CAT beamline 24-ID-E at the Advanced Photon Source of Argonne National Laboratory.

ABBREVIATIONS

pol	polymerase
exo	exonuclease
RB69pol	RB69 DNA polymerase
NBP	Nascent Base-pair binding Pocket
P/T	primer/template
W-C	Watson-Crick
wt	wild type
BP	Base-pair
HB	hydrogen bond or hydrogen bonding
KF	Klenow Fragment
tC°	1,3,-diaza-2 oxophenoxazine
2AP	2-aminopurine
$\mathbf{K_{d,net}}$ =	$K_{d,1}/(1+K_2)$ without chemistry
$\mathbf{K_{d,app}}$ =	[dNTP] that gives a k_{obs} that is half the maximum rate, k_{pol}
$\mathbf{K_{d,1}}$ =	k_{-1}/k_1
$\mathbf{K_2}$ =	k_2/k_{-2}

REFERENCES

(1). Drake JW. Comparative rates of spontaneous mutation. Nature. 1969; 221:1132. [PubMed: 4378427]

(2). Echols H, Goodman MF. Fidelity mechanisms in DNA replication. Annu Rev Biochem. 1991; 60:477–511. [PubMed: 1883202]

(3). Kunkel TA, Bebenek K. DNA replication fidelity. Annu Rev Biochem. 2000; 69:497–529. [PubMed: 10966467]

(4). Kunkel TA. DNA replication fidelity. J Biol Chem. 2004; 279:16895–16898. [PubMed: 14988392]

(5). Brutlag D, Kornberg A. Enzymatic synthesis of deoxyribonucleic acid. 36. A proofreading function for the 3' leads to 5' exonuclease activity in deoxyribonucleic acid polymerases. J Biol Chem. 1972; 247:241–248. [PubMed: 4336040]

(6). Muzyczka N, Poland RL, Bessman MJ. Studies on the biochemical basis of spontaneous mutation. I. A comparison of the deoxyribonucleic acid polymerases of mutator, antimutator, and wild type strains of bacteriophage T4. J Biol Chem. 1972; 247:7116–7122. [PubMed: 4565077]

(7). Kunkel TA. Exonucleolytic proofreading. Cell. 1988; 53:837–840. [PubMed: 2838173]

(8). Capson TL, Peliska JA, Kaboord BF, Frey MW, Lively C, Dahlberg M, Benkovic SJ. Kinetic characterization of the polymerase and exonuclease activities of the gene 43 protein of bacteriophage T4. Biochemistry. 1992; 31:10984–10994. [PubMed: 1332748]

(9). Franklin MC, Wang J, Steitz TA. Structure of the replicating complex of a pol alpha family DNA polymerase. Cell. 2001; 105:657–667. [PubMed: 11389835]

(10). Purohit V, Grindley ND, Joyce CM. Use of 2-aminopurine fluorescence to examine conformational changes during nucleotide incorporation by DNA polymerase I (Klenow fragment). Biochemistry. 2003; 42:10200–10211. [PubMed: 12939148]

(11). Hariharan C, Reha-Krantz LJ. Using 2-aminopurine fluorescence to detect bacteriophage T4 DNA polymerase-DNA complexes that are important for primer extension and proofreading reactions. Biochemistry. 2005; 44:15674–15684. [PubMed: 16313170]

(12). Hariharan C, Bloom LB, Helquist SA, Kool ET, Reha-Krantz LJ. Dynamics of nucleotide incorporation: snapshots revealed by 2-aminopurine fluorescence studies. Biochemistry. 2006; 45:2836–2844. [PubMed: 16503638]

(13). Tsai YC, Johnson KA. A new paradigm for DNA polymerase specificity. Biochemistry. 2006; 45:9675–9687. [PubMed: 16893169]

(14). Zhang H, Cao W, Zakharova E, Konigsberg W, De La Cruz EM. Fluorescence of 2-aminopurine reveals rapid conformational changes in the RB69 DNA polymerase-primer/template complexes upon binding and incorporation of matched deoxynucleoside triphosphates. Nucleic Acids Res. 2007; 35:6052–6062. [PubMed: 17766250]

(15). Wang M, Xia S, Blaha G, Steitz TA, Konigsberg WH, Wang J. Insights into base selectivity from the 1.8 A resolution structure of an RB69 DNA polymerase ternary complex. Biochemistry. 2011; 50:581–590. [PubMed: 21158418]

(16). Xia S, Wang M, Blaha G, Konigsberg WH, Wang J. Structural Insights into Complete Metal Ion Coordination from Ternary Complexes of B Family RB69 DNA Polymerase. Biochemistry. 2011; 50:9114–9124. [PubMed: 21923197]

(17). Joyce CM, Steitz TA. Function and structure relationships in DNA polymerases. Annu Rev Biochem. 1994; 63:777–822. [PubMed: 7526780]

(18). Joyce CM, Benkovic SJ. DNA polymerase fidelity: kinetics, structure, and checkpoints. Biochemistry. 2004; 43:14317–14324. [PubMed: 15533035]

(19). Bakhtina M, Roettger MP, Kumar S, Tsai MD. A unified kinetic mechanism applicable to multiple DNA polymerases. Biochemistry. 2007; 46:5463–5472. [PubMed: 17419590]

(20). Johnson KA. Role of induced fit in enzyme specificity: a molecular forward/reverse switch. J Biol Chem. 2008; 283:26297–26301. [PubMed: 18544537]

(21). Johnson KA. The kinetic and chemical mechanism of high-fidelity DNA polymerases. Biochim Biophys Acta. 2010; 1804:1041–1048. [PubMed: 20079883]

(22). Frey MW, Sowers LC, Millar DP, Benkovic SJ. The nucleotide analog 2-aminopurine as a spectroscopic probe of nucleotide incorporation by the Klenow fragment of Escherichia coli polymerase I and bacteriophage T4 DNA polymerase. Biochemistry. 1995; 34:9185–9192. [PubMed: 7619819]

(23). Fidalgo da Silva E, Mandal SS, Reha-Krantz LJ. Using 2-aminopurine fluorescence to measure incorporation of incorrect nucleotides by wild type and mutant bacteriophage T4 DNA polymerases. J Biol Chem. 2002; 277:40640–40649. [PubMed: 12189135]

(24). Mandal SS, Fidalgo da Silva E, Reha-Krantz LJ. Using 2-aminopurine fluorescence to detect base unstacking in the template strand during nucleotide incorporation by the bacteriophage T4 DNA polymerase. Biochemistry. 2002; 41:4399–4406. [PubMed: 11914087]

(25). Beckman J, Wang M, Blaha G, Wang J, Konigsberg WH. Substitution of Ala for Tyr567 in RB69 DNA polymerase allows dAMP to be inserted opposite 7,8-dihydro-8-oxoguanine. Biochemistry. 2010; 49:4116–4125. [PubMed: 20411947]

(26). Beckman J, Wang M, Blaha G, Wang J, Konigsberg WH. Substitution of Ala for Tyr567 in RB69 DNA polymerase allows dAMP and dGMP to be inserted opposite Guanidinohydantoin. Biochemistry. 2010; 49:8554–8563. [PubMed: 20795733]

(27). Xia S, Konigsberg WH, Wang J. Hydrogen-bonding capability of a templating difluorotoluene nucleotide residue in an RB69 DNA polymerase ternary complex. J Am Chem Soc. 2011; 133:10003–10005. [PubMed: 21667997]

(28). Xia S, Eom SH, Konigsberg WH, Wang J. Structural Basis for Differential Insertion Kinetics of dNMPs Opposite a Difluorotoluene Nucleotide Residue. Biochemistry. 2012; 51:1476–1485. [PubMed: 22304682]

(29). Reha-Krantz LJ, Hariharan C, Subuddhi U, Xia S, Zhao C, Beckman J, Christian T, Konigsberg W. Structure of the 2-aminopurine-cytosine base pair formed in the polymerase active site of the RB69 Y567A-DNA polymerase. Biochemistry. 2011; 50:10136–10149. [PubMed: 22023103]

(30). Engman KC, Sandin P, Osborne S, Brown T, Billeter M, Lincoln P, Norden B, Albinsson B, Wilhelmsson LM. DNA adopts normal B-form upon incorporation of highly fluorescent DNA base analogue tC: NMR structure and UV-Vis spectroscopy characterization. Nucleic Acids Res. 2004; 32:5087–5095. [PubMed: 15452275]

(31). Stengel G, Gill JP, Sandin P, Wilhelmsson LM, Albinsson B, Norden B, Millar D. Conformational dynamics of DNA polymerase probed with a novel fluorescent DNA base analogue. Biochemistry. 2007; 46:12289–12297. [PubMed: 17915941]

(32). Magat Juan EC, Shimizu S, Ma X, Kurose T, Haraguchi T, Zhang F, Tsunoda M, Ohkubo A, Sekine M, Shibata T, Millington CL, Williams DM, Takenaka A. Insights into the DNA stabilizing contributions of a bicyclic cytosine analogue: crystal structures of DNA duplexes containing 7,8-dihydropyrido [2,3-d]pyrimidin-2-one. Nucleic Acids Res. 2010; 38:6737–6745. [PubMed: 20554855]

(33). Preus S, Borjesson K, Kilsa K, Albinsson B, Wilhelmsson LM. Characterization of nucleobase analogue FRET acceptor tCnitro. J Phys Chem B. 2010; 114:1050–1056. [PubMed: 20039634]

(34). Wilhelmsson LM. Fluorescent nucleic acid base analogues. Q Rev Biophys. 2010; 43:159–183. [PubMed: 20478079]

(35). Sandin P, Wilhelmsson LM, Lincoln P, Powers VE, Brown T, Albinsson B. Fluorescent properties of DNA base analogue tC upon incorporation into DNA--negligible influence of neighbouring bases on fluorescence quantum yield. Nucleic Acids Res. 2005; 33:5019–5025. [PubMed: 16147985]

(36). Sandin P, Borjesson K, Li H, Martensson J, Brown T, Wilhelmsson LM, Albinsson B. Characterization and use of an unprecedentedly bright and structurally non-perturbing fluorescent DNA base analogue. Nucleic Acids Res. 2008; 36:157–167. [PubMed: 18003656]

(37). Stengel G, Purse BW, Wilhelmsson LM, Urban M, Kuchta RD. Ambivalent incorporation of the fluorescent cytosine analogues tC and tCo by human DNA polymerase alpha and Klenow fragment. Biochemistry. 2009; 48:7547–7555. [PubMed: 19580325]

(38). Zhang H, Beckman J, Wang J, Konigsberg W. RB69 DNA polymerase mutants with expanded nascent base-pair-binding pockets are highly efficient but have reduced base selectivity. Biochemistry. 2009; 48:6940–6950. [PubMed: 19522539]

(39). Xia S, Wang M, Lee HR, Sinha A, Blaha G, Christian T, Wang J, Konigsberg W. Variation in mutation rates caused by RB69pol fidelity mutants can be rationalized on the basis of their kinetic behavior and crystal structures. J Mol Biol. 2011; 406:558–570. [PubMed: 21216248]

(40). Xia S, Eom SH, Konigsberg WH, Wang J. Bidentate and tridentate metal-ion coordination states within ternary complexes of RB69 DNA polymerase. Protein Sci. 2012; 21:447–451. [PubMed: 22238207]

(41). Zhang H, Rhee C, Bebenek A, Drake JW, Wang J, Konigsberg W. The L561A substitution in the nascent base-pair binding pocket of RB69 DNA polymerase reduces base discrimination. Biochemistry. 2006; 45:2211–2220. [PubMed: 16475809]

(42). Maniatis, T.; Fritsch, EF.; Sambrook, J., editors. Molecular cloning: a laboratory nanual. Cold spring harbor laboratory press; Plainview: 1982.

(43). Kuchta RD, Mizrahi V, Benkovic PA, Johnson KA, Benkovic SJ. Kinetic mechanism of DNA polymerase I (Klenow). Biochemistry. 1987; 26:8410–8417. [PubMed: 3327522]

(44). Otwinowski, Z.; Minor, W. Processing of X-ray diffraction data collected in oscillation mode. In: Carter, CW.; Sweet, RM., editors. Methods in Enzymology. 1997. p. 307-326.

(45). Murshudov GN, Vagin AA, Dodson EJ. Refinement of macromolecular structures by the maximum-likelihood method. Acta Cryst. 1997; D53:240–255.

(46). Navaza J. Acta Cryst. 1994; A50:157–163.

(47). Emsley P, Cowtan K. Coot: model-building tools for molecular graphics. Acta Cryst. 2004; D60:2126–2132.

(48). Version 1.2r3pre. Schrodinger, LLC; The PyMOL Molecular Graphics System.

(49). Lee HR, Wang M, Konigsberg W. The reopening rate of the fingers domain is a determinant of base selectivity for RB69 DNA polymerase. Biochemistry. 2009; 48:2087–2098. [PubMed: 19228036]

(50). Rothwell PJ, Mitaksov V, Waksman G. Motions of the fingers subdomain of klentaq1 are fast and not rate limiting: implications for the molecular basis of fidelity in DNA polymerases. Mol Cell. 2005; 19:345–355. [PubMed: 16061181]

(51). Christian TD, Romano LJ, Rueda D. Single-molecule measurements of synthesis by DNA polymerase with base-pair resolution. Proc Natl Acad Sci U S A. 2009; 106:21109–21114. [PubMed: 19955412]

(52). Braithwaite DK, Ito J. Compilation, alignment, and phylogenetic relationships of DNA polymerases. Nucleic Acids Res. 1993; 21:787–802. [PubMed: 8451181]

$$ED_n + dNTP \underset{k_{-1}}{\overset{k_1}{\rightleftharpoons}} ED_n dNTP \underset{k_{-2}}{\overset{k_2}{\rightleftharpoons}} FD_n dNTP \underset{k_{-3}}{\overset{k_3}{\rightleftharpoons}} FD_{n+1} PPi \xrightarrow{k_4} ED_{n+1} + PPi$$

Scheme I.

Pathway of dNTP binding and incorporation. ED_n is the open complex, and FD_n is the closed complex.

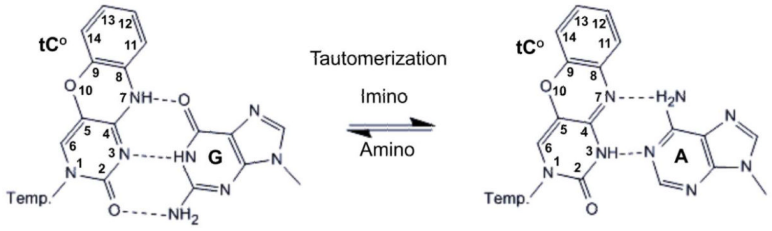

Figure 1.
Pairing of guanine (G) and adenine (A) opposite tC°. The analogue pairs with adenine upon tautomerization to the imino form.

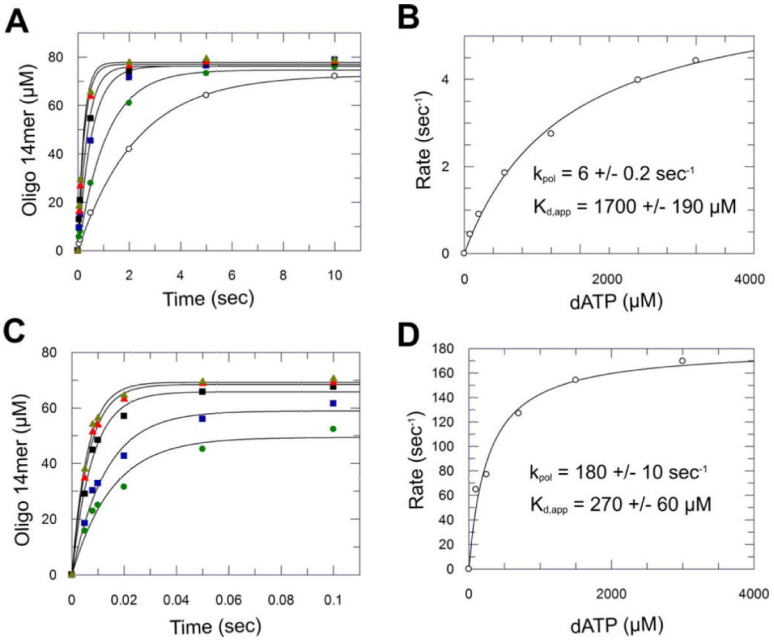

Figure 2.

Kinetic insertion of dAMP opposite tC° by the wt (A–B) and the Y567A mutant (C–D). (A) Progress curves at various dATP concentrations, 100, 250, 700, 1500, 3000, and 4000 μM (from bottom to top), fit to a single-exponential equation. (B) Plot of k_{obs} vs [dATP] fit to hyperbolic equation to yield k_{pol} and $K_{d,app}$. (C) Progress curves at various dATP concentrations, 100, 250, 700, 1500, and 3000 μM (from bottom to top), fit to a single-exponential equation. (D) Plot of k_{obs} vs [dATP] fit to hyperbolic equation to yield k_{pol} and $K_{d,app}$.

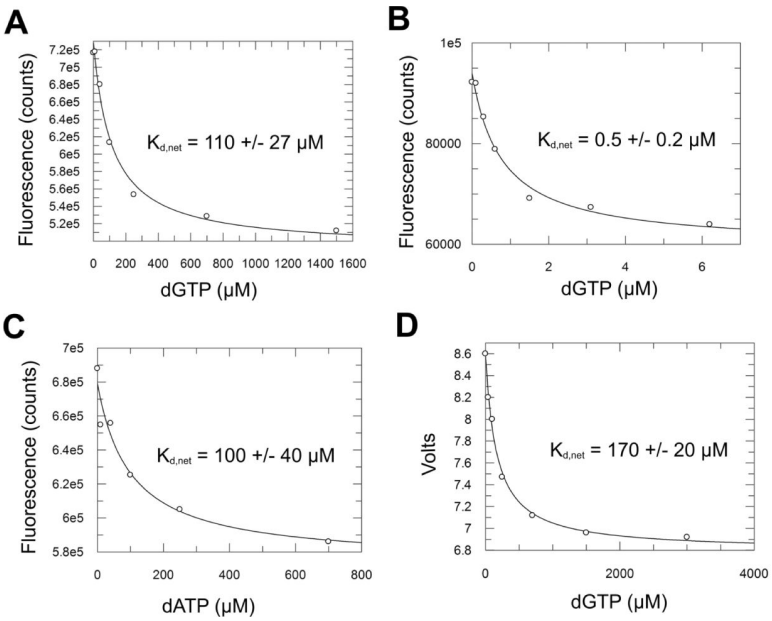

Figure 3.

Results of fluorescence titrations of dNTPs opposite tC° in P/T complexes with the wt and the Y567A mutant: (A) Dissociation constants (K*d,net*) for dGTP binding opposite tC° in the wt ternary complex; (B) dGTP binding opposite tC° in the Y567A mutant ternary complex; (C) dATP binding opposite tC° in the Y567A mutant ternary complex. (D) A plot of amplitude changes obtained by stopped-flow fluorescence for dGTP opposite tC° with wt RB69pol.

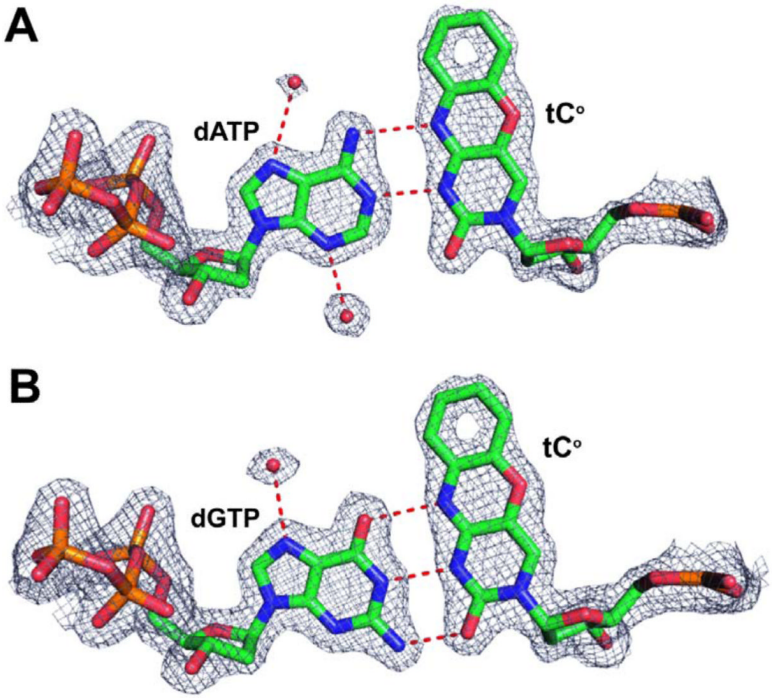

Figure 4.

The structures of dNTP/tC° nascent base pairs in the ternary complexes of RB69pol Y567A mutant. (A) Final 2Fo-Fc electron desnity map at 1.88 Å resolution for the dATP/tC° containing complex contoured at 1.8 σ. (B) Final 2Fo-Fc electron desnity map at 1.92 Å resolution for the dGTP/tC° containing complex contoured at 1.8 σ.

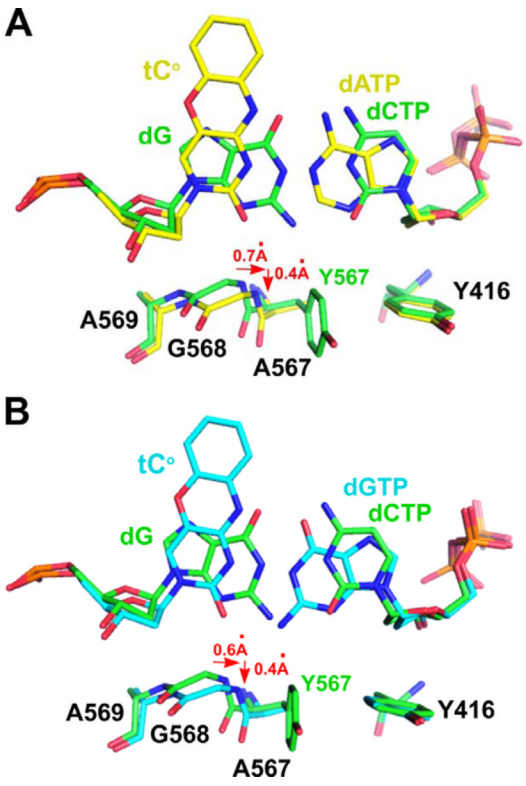

Figure 5.
(A) Superposition of the dATP/tC°-containing Y567A mutant ternary complex (yellow) with the dCTP/dG-containing wt ternary complex (green). (B) Superposition of the dGTP/tC °-containing Y567A mutant ternary complex (cyan) with the dCTP/dG-containing wt ternary complex (green).

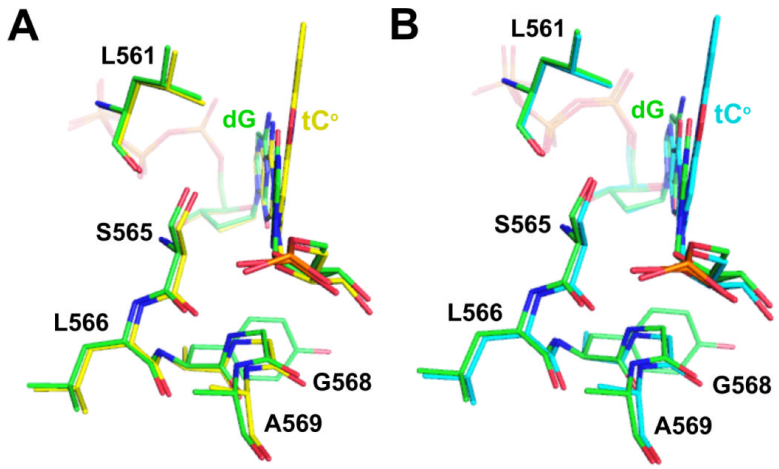

Figure 6.

(A) Superposition of the dATP/tC°-containing Y567A mutant ternary complex (yellow) with the dCTP/dG-containing wt ternary complex (green). (B) Superposition of the dGTP/tC °-containing Y567A mutant ternary complex (cyan) with the dCTP/dG-containing wt ternary complex (green).

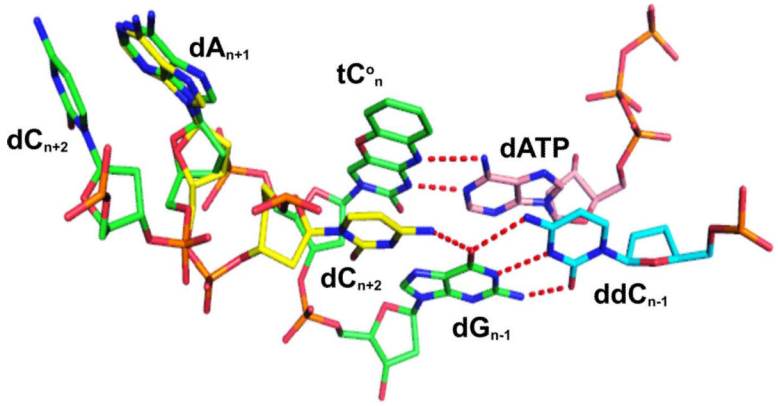

Figure 7.
Two alternative conformations of the 5' overhang of the template strand in the dATP/tC°-containing Y567A mutant ternary complex. The template strand is shown in green. The overhanging DNA in the alternative conformation is shown in yellow.

Table 1

Crystallographic statistics for data collection and refinement of the tC°/dNTP-containing ternary complexes of the RB69pol Y567A mutant

dNTP/tC°	dATP/ tC°	dGTP/tC°
Space group	$P2_12_12_1$	$P2_12_12_1$
Unit cell dimensions [a,b,c (Å)]	74.9, 120.5, 130.9	74.8, 120.0, 130.0
Resolution range (Å)	50.0 – 1.88	50.0 – 1.92
Number of reflections		
Unique	90492	85100
Redundancy	4.0 (3.2)	4.7 (3.4)
Completeness (%)	99.5 (93.8)	99.6 (96.2)
R_{merge} (%)	6.3 (50.7)	10.1 (95.1)
I/σ	18.3 (1.6)	14.4 (1.4)
Final model		
Amino acid residues	903	903
Water molecules	1001	786
Ca^{2+} ions	4	7
Template nucleotides	18	18
Primer nucleotides	13	13
dNTP molecules	1	1
Refinement Statistics		
Reflections	95575	90003
R_{work} (%)	17.4 (26.9)	18.0 (29.8)
R_{free} (%)	21.2 (30.5)	21.3 (34.6)
r.m.s.d.		
Bond length (Å)	0.007	0.008
Bond angle (°)	1.137	1.134
PDB code	3QNO	3QNN

Footnotes:

a, Statistics for the highest resolution shell are in parenthesis.

b, $R_{merge} = \Sigma_{hkl}\Sigma_j|I_j(hkl) - \langle I_j(hkl)\rangle|/\Sigma_{hkl}\,\Sigma_j \langle I(hkl)\rangle$, statistics for merging all observations for given reflections.

c, $R = \Sigma_{hkl}|F_{obs}(hkl) - F_{calc}(hkl)|/\Sigma_{hkl}\,F_{obs}(hkl)$, statistics for crystallographic agreement between the measured and model-calculated amplitudes. Rfree is the agreement for cross-validation data set.

e, Root mean squares deviations (rmsd) to ideal values.

Table 2

Pre-steady-state kinetic parameters for incorporation of dAMP and dGMP opposite tC° by wt RB69pol and the Y567A mutant.

RB69pol	dNTP	Template	k_{pol} (s^{-1})	$K_{d,app}$ (μM)	$K_{pol}/K_{d,app}$ ($\mu M^{-1}s^{-1}$)
wt	dATP	tC°	6 ± 0.2	1700 ± 190	3.5×10^{-3}
	dGTP	tC°	250 ± 7	140 ± 18	1.8
Y567A	dATP	tC°	180 ± 10	270 ± 60	0.7
	dGTP	tC°	170 ± 10	4 ± 1	43

Table 3

Fluorescence titration of dGTP and dATP opposite tC° by wt RB69pol and the Y567A mutant.

RB69pol	dNTP	$K_{d,net}$ (μM)
wt	dGTP	110 ± 27
Y567A	dGTP	0.5 ± 0.2
	dATP	100 ± 40